THE JOURNAL OF BIOLOGICAL CHEMISTRY VOL. 287, NO. 35, pp. 29506–29515, August 24, 2012


# The Roles of the Dimeric and Tetrameric Structures of the Clock Protein KaiB in the Generation of Circadian Oscillations in Cyanobacteria*[S]

Received for publication, February 3, 2012, and in revised form, June 19, 2012 Published, JBC Papers in Press, June 21, 2012, DOI 10.1074/jbc.M112.349092

**Reiko Murakami**[‡1,2], **Risa Mutoh**[‡§1,3,4], **Ryo Iwase**[‡§], **Yukio Furukawa**[¶], **Katsumi Imada**[¶3,5], **Kiyoshi Onai**[‡], **Megumi Morishita**[‡], **So Yasui**[‡§], **Kentaro Ishii**[‡3], **Jonathan Orville Valencia Swain**[‡§], **Tatsuya Uzumaki**[§], **Keiichi Namba**[¶], **and Masahiro Ishiura**[‡§6]

*From the* [‡]*Center for Gene Research and* [§]*Division of Biological Science, Graduate School of Science, Nagoya University, Furo, Chikusa, Nagoya 464-8602, Japan and* [¶]*Graduate School of Frontier Biosciences, Osaka University, 1-3 Yamadaoka, Suita, Osaka 565-0871, Japan*

**Background:** The function of KaiB remains to be solved.
**Results:** Dimeric $KaiB_{1-94}$ generated circadian oscillation *in vitro*, but it did not in cells.
**Conclusion:** KaiB tetramer-dimer transformation is responsible for the regulation of the SasA-mediated clock output pathway.
**Significance:** We demonstrated the role of KaiB in the regulation of the SasA-KaiC interaction, involved in the transmission of time-information from KaiABC-machinery to transcription apparatus.

**The molecular machinery of the cyanobacterial circadian clock consists of three proteins, KaiA, KaiB, and KaiC. The three Kai proteins interact with each other and generate circadian oscillations *in vitro* in the presence of ATP (an *in vitro* KaiABC clock system). KaiB consists of four subunits organized as a dimer of dimers, and its overall shape is that of an elongated hexagonal plate with a positively charged cleft flanked by two negatively charged ridges. We found that a mutant KaiB with a C-terminal deletion ($KaiB_{1-94}$), which lacks the negatively charged ridges, was a dimer. Despite its dimeric structure, $KaiB_{1-94}$ interacted with KaiC and generated normal circadian oscillations in the *in vitro* KaiABC clock system. $KaiB_{1-94}$ also generated circadian oscillations in cyanobacterial cells, but they were weak, indicating that the C-terminal region and tetrameric structure of KaiB are necessary for the generation of normal gene expression rhythms *in vivo*. $KaiB_{1-94}$ showed the highest affinity for KaiC among the KaiC-binding proteins we examined and inhibited KaiC from forming a complex with SasA, which is involved in the main output pathway from the KaiABC clock oscillator in transcription regulation. This defect explains the mechanism underlying the lack of normal gene expression rhythms in cells expressing $KaiB_{1-94}$.**

The circadian clock is an endogenous biological mechanism that generates daily cycles in physiological activity (circadian rhythms) (1, 2). Cyanobacteria are the simplest organisms that exhibit circadian rhythms (2), and the circadian clock gene cluster *kaiABC* is essential for circadian rhythms in cyanobacteria (3). The rhythms involve circadian oscillations in the phosphorylation level (4) and ATPase activity (5) of KaiC and complex formation among KaiA, KaiB, and KaiC (6, 7). KaiC has a duplicated RecA/DnaB structure. Its N-terminal domain shows ATPase activity (8), whereas its C-terminal domain shows both ATPase activity (5, 8) and intersubunit phosphorylation activity (9, 10). KaiA and KaiB have opposite effects on KaiC ATPase activity (5, 8) and phosphorylation level; KaiA increases them (10–13), and KaiB decreases them (5, 12, 14). KaiB is composed of two asymmetric dimers (15, 16) that form a tetramer. KaiB directly associates with the C-terminal clock oscillator domain (13) of KaiA (17). Its overall shape is that of an elongated hexagonal plate with a positively charged cleft (PC)[7] that is flanked by two negatively charged ridges (NRs) (16). Rhythm analysis of cyanobacterial cells carrying a mutant *kaiB* gene show that the PC is necessary to KaiB clock function (16). Deletion of the C-terminal residues from amino acids 95–108 of KaiB (yielding mutant $KaiB_{1-94}$) derived from the cyanobac-

* This work was supported by grants from the Ministry of Education, Culture, Sports, Science, and Technology of Japan (to M. I. and K. O.).
[S] This article contains supplemental Figs. S1–S3.
[1] Both authors contributed equally to this work.
[2] Supported by a grant from Leavanest and MBL (Tokyo, Japan).
[3] Research assistants supported by a Global Center of Excellence grant from Ministry of Education, Culture, Sports, Science, and Technology of Japan.
[4] Supported by grants from Research Fellowships of the Japan Society for the Promotion of Science for Young Scientists. Present address: Institute for Protein Research, Osaka University, 3-2 Yamadaoka, Suita, Osaka 565-0871, Japan.
[5] Present address: Graduate School of Sciences, Osaka University, 1-1 Machikaneyama, Toyonaka, Osaka 560-0043, Japan.
[6] To whom correspondence should be addressed: Division of Biological Science, Graduate School of Science, Nagoya University, Furo, Chikusa, Nagoya 464-8602, Japan. Tel.: 81-52-789-4527; Fax: 81-52-789-4526; E-mail: ishiura@gene.nagoya-u.ac.jp.

[7] The abbreviations used are: PC, the positively charged cleft of KaiB; NRs, the two negatively charged ridges of KaiB; p-KaiC, phosphorylated KaiC; CBB, Coomassie Brilliant Blue; FCS, fluorescence correlation spectroscopy; $KaiB_{1-94}$, a truncated mutant KaiB with a C-terminal deletion from residues 95 to 108; $KaiB_{WT}$, wild-type KaiB; $KaiC_{AA}$, a mutant KaiC with alanine substitutions at the two KaiC phosphorylation sites; $KaiC_{DD}$, a mutant KaiC with aspartate substitutions at the two KaiC phosphorylation sites; np-KaiC, nonphosphorylated KaiC; $K_D$, apparent equilibrium dissociation constant; *Synechococcus*, *Synechococcus* sp. strain PCC 7942.

teria *Synechococcus* sp. strain PCC 7942 (hereafter *Synechococcus*) and *Thermosynechococcus elongatus* results in loss of the NRs and extensively weakens *in vivo* circadian rhythms (16). Here we examine the structure of $KaiB_{1-94}$ and the role it plays in the generation circadian oscillations.

## EXPERIMENTAL PROCEDURES

*Protein Expression and Purification*—KaiA, KaiB, KaiC, and SasA derived from *T. elongatus* (18) were expressed in *Escherichia coli* BL21 cells and purified as previously described (16, 17, 19–21). We generated gene constructs for a truncated mutant KaiB with a C-terminal deletion from residues 95–108 ($KaiB_{1-94}$) and a mutant KaiC with alanine ($KaiC_{AA}$) or aspartate ($KaiC_{DD}$) substitutions at the two KaiC phosphorylation sites using PCR-mediated site-directed mutagenesis and cloned them in the pGEX-6P-1 vector (GE Healthcare) as described previously (20).

To determine their purity, we subjected the purified proteins to SDS-PAGE on 15% gels (22) and stained the gels with Coomassie Brilliant Blue (CBB). We estimated protein concentrations using the Bio-Rad Protein Assay with BSA as the standard as previously described (20). Unless otherwise stated, KaiA, KaiB, KaiC, and SasA refer to the KaiA dimer, KaiB tetramer, KaiC hexamer, and SasA trimer (21), respectively, and their concentrations are expressed in terms of their oligomeric status.

*Estimation of the Molecular Mass of KaiB by Gel Filtration Chromatography*—We estimated the molecular mass of KaiB using analytical gel filtration chromatography on a Superdex 75 5/150GL column (GE Healthcare) equilibrated with 20 mM Tris-HCl buffer (pH 7.5) containing 150 mM NaCl (gel filtration buffer) at 4 °C using an ÄKTA explorer (GE Healthcare) and a Gel Filtration Calibration Kit LMW (GE Healthcare) for the molecular mass standards. We monitored the elution profiles of proteins by absorbance at 280 nm ($A_{280}$) and performed all analyses in 20 mM Tris-HCl buffer (pH 7.5) containing 50 mM NaCl, 20 mM Tris-HCl buffer (pH 7.5) containing 500 mM NaCl, 20 mM MES-NaOH buffer (pH 6.5) containing 150 mM NaCl, and 20 mM Tris-HCl buffer (pH 8.5) containing 150 mM NaCl.

*Sedimentation Equilibrium by Analytical Ultracentrifugation*—We performed sedimentation equilibrium analytical ultracentrifugation using a Beckman Optima XL-A analytical ultracentrifuge with an An60Ti rotor. Samples were dialyzed against 20 mM HEPES-NaOH buffer (pH 7.5) containing 150 mM NaCl (sedimentation equilibrium buffer), which was used as the blank. We performed measurements at 20 °C at 36,000, 38,000, and 40,000 rpm for $KaiB_{1-94}$ and at 20,000, 22,000, and 24,000 rpm for wild-type KaiB ($KaiB_{WT}$). We monitored concentration profiles of the samples by $A_{280}$ and recorded them at a spacing of 0.001 cm in step mode, with 20 averages per step. We analyzed equilibrium data with Beckman Optima XL-A/XL-I data analyses software, Version 6.04, which was provided as an add-on to Version 6.0 (Microcal Inc.), and we calculated global, single-species fits using different loading absorbance values at 280 nm (0.2, 0.25, and 0.3 for $KaiB_{1-94}$ and 0.18 for $KaiB_{WT}$). Based on the amino acid compositions of the proteins, we used the partial specific volumes 0.767 ml/g for $KaiB_{1-94}$ and 0.759 ml/g for $KaiB_{WT}$ for the analyses.

*Estimation of the Molecular Mass and Stoichiometry of the KaiB-KaiC Complex by Gel Filtration Chromatography*—Reaction mixtures containing 5 $\mu$M $KaiB_{1-94}$ or 2.5 $\mu$M $KaiB_{WT}$ and 1 $\mu$M $KaiC_{DD}$ in 20 mM HEPES-NaOH buffer (pH 7.5) containing 1 mM ATP, 5 mM $MgCl_2$, and 150 mM NaCl (HEPES reaction buffer) were incubated at 40 °C for 18 h and analyzed by gel filtration chromatography on a Superdex 200/HR 10/300 column (GE Healthcare) equilibrated with HEPES reaction buffer containing 0.1 mM ATP and 5 mM $MgCl_2$ at 4 °C. We used thyroglobulin (670 kDa), apoferritin (440 kDa), $\beta$-amylase (200 kDa), and BSA (66 kDa) as molecular mass standards. Fractions containing the KaiB-$KaiC_{DD}$ complex were subjected to SDS-PAGE on 18% gels, and then the gels were stained with CBB. We determined the amount of KaiB and $KaiC_{DD}$ contained in the complex by densitometry using a CS analyzer (ATTO) to determine the stoichiometry of the complex.

*Labeling of KaiB with Cy3 and Fluorescence Correlation Spectroscopy (FCS) Measurements*—Cy3-NHS fluorescent dye esters (GE Healthcare) were covalently coupled to the amines of lysine residues and the N-terminal amino acid residue of KaiB. KaiB (8 $\mu$M $KaiB_{1-94}$ or 4 $\mu$M $KaiB_{WT}$) was incubated with 80 $\mu$M Cy3-NHS ester in gel filtration buffer at 4 °C for 2 h. After labeling, the reaction mixtures were loaded on a PD MidiTrap™ G-25 column (GE Healthcare) for removal of the remaining unbound dye from the labeled proteins. We calculated the amounts of Cy3 introduced onto KaiB from the absorbance of the labeled proteins at 552 nm ($A_{552}$). Under these conditions, 0.85 ± 0.10 and 0.64 ± 0.01 molecules of Cy3 ($n = 3$) per subunit of $KaiB_{1-94}$ and $KaiB_{WT}$ were introduced into $KaiB_{1-94}$ and $KaiB_{WT}$, respectively.

We performed FCS measurements using a multiphoton FCS/fluorescence cross-correlation spectroscopy system using Fluctuation Dual Emission Uni-laser eXcitation (Fluc DEUX™) (MBL, Nagoya, Japan). Cy3 was excited by the 445-nm laser, and its emission was detected at 615–690 nm. Cy3-$KaiB_{1-94}$ and Cy3-$KaiB_{WT}$ (0.1 $\mu$M) were separately incubated with 0, 0.03, 0.05, 0.10, and 0.30 $\mu$M $KaiC_{DD}$ in the presence of 0, 0.05, 0.10, or 0.30 $\mu$M SasA in HEPES reaction buffer at 25 °C for 18 h, and the reaction mixtures were subjected to FCS measurements at 25 °C for 5 s (5 times consecutively). The diffusion time defined as the average time required for the diffusion of fluorescent particles across the detection area reflects the size of the particles. If the effect of the molecular shape on its diffusion is negligible, diffusion time is proportional to the cubic root of the molecular mass, as described in Equation 1 (23, 24),

$$DT_a/DT_b = \sqrt[3]{MM_a/MM_b}, \quad \text{(Eq. 1)}$$

where $DT_a$ and $DT_b$ are the diffusion times of molecules a (Cy3-$KaiB_{1-94}$ or Cy3-$KaiB_{WT}$) and b (Cy3-$KaiB_{1-94}$-$KaiC_{DD}$ complex or Cy3-$KaiB_{WT}$-$KaiC_{DD}$), respectively, and $MM_a$ and $MM_b$ are the molecular masses of molecules a and b, respectively. Accordingly, we calculated the size of the Cy3-$KaiB_{1-94}$-$KaiC_{DD}$ and Cy3-$KaiB_{WT}$-$KaiC_{DD}$ complexes to be 320 ± 70 and 370 ± 90 kDa, respectively, using the molecular masses of Cy3-$KaiB_{WT}$ (~50 kDa) and Cy3-$KaiB_{1-94}$ (~25 kDa). These

values are consistent with the molecular masses determined by gel filtration chromatography (see Fig. 2*A*).

*Surface Plasmon Resonance Analysis of Interaction between KaiB and KaiC*—We analyzed the interaction between $KaiB_{1-94}$ and $KaiC_{DD}$ and between $KaiB_{WT}$ and $KaiC_{DD}$ at 25 °C by surface plasmon resonance (25) using a Biacore and its associated software (GE Healthcare). $KaiC_{DD}$ (10 $\mu$M) was immobilized on a CM5 sensor chip using an amine coupling kit (GE Healthcare) in HEPES reaction buffer containing 0.1 mM ATP, 0.1 mM dithiothreitol (DTT), and 50 mM NaCl. We monitored the association to, and dissociation from, the immobilized $KaiC_{DD}$ of $KaiB_{1-94}$, $KaiB_{WT}$, KaiA, and SasA continuously at stepwise concentrations of 0.1, 0.25, 0.5, 1.0, and 1.5 $\mu$M in HEPES reaction buffer. We computed the dissociation ($k_d$) and association ($k_a$) rates by fitting a 1:1 binding model to the experimental data. We calculated the value for apparent equilibrium dissociation constant ($K_D$) as $k_d/k_a$.

*Measurement of the Phosphorylation Levels of KaiC*—Reaction mixtures of KaiA and KaiC (each 0.5 $\mu$M) were incubated in the presence or absence of 1.0 $\mu$M $KaiB_{1-94}$ or 0.5 $\mu$M $KaiB_{WT}$ in gel filtration buffer containing 1 mM ATP and 5 mM $MgCl_2$ at 25 or 40 °C, and 10-$\mu$l aliquots of the reaction mixtures were removed to stop the reaction at specific time intervals. The aliquots were subjected to SDS-PAGE on 12.5% gels (acrylamide:bisacrylamide = 144:1), and the gels were stained with CBB. The intensities of bands were measured by densitometry using a CS Analyzer. KaiC showed a triplet band on SDS-PAGE (4, 9); the two upper bands correspond to phosphorylated KaiC (p-KaiC), and the lowest band corresponds to nonphosphorylated KaiC (np-KaiC). We calculated the relative amount of p-KaiC to total KaiC (the level of p-KaiC) from band intensities and analyzed the circadian oscillations of the level of p-KaiC using the program RAP (26).

*In Vivo Bioluminescence Rhythm Assay*—We measured the bioluminescence rhythms of the *T. elongatus* strains carrying a $P_{psbA1}$::Xl *luxAB* reporter gene at 41 °C using a newly developed bioluminescence monitoring apparatus with a robotic plate conveyor. The apparatus was 1.3 times as sensitive to luminescence as our previous apparatuses (27). We analyzed bioluminescence data by a modified cosiner method of RAP as previously described (26, 28). We examined the wild-type strain, a *kaiB*-null strain carrying a mutant *kaiB* gene with a nonsense mutation downstream of its initiation codon, and a strain carrying an additional mutant *kaiB* gene encoding $KaiB_{1-94}$, $kaiB_{1-94}$, in the *kaiB*-null genetic background (16, 29).

*Assay for the Complex Formation of SasA with KaiC by Gel Filtration Chromatography*—Reaction mixtures containing 1.5 $\mu$M SasA and 0.6 $\mu$M $KaiC_{DD}$ were incubated in the presence or absence of 3.0 $\mu$M $KaiB_{WT}$ or 6.0 $\mu$M $KaiB_{1-94}$ in HEPES reaction buffer containing 0.1 mM DTT at 25 °C for 18 h and analyzed by gel filtration chromatography on a Superdex 200/HR 10/300 column (GE Healthcare) equilibrated with HEPES reaction buffer containing 0.1 mM ATP, 5 mM $MgCl_2$, and 0.1 mM DTT at 4 °C. Aliquots of the chromatography fractions were subjected to SDS-PAGE on 15% gels, and the gels were stained with CBB. We determined the amount of SasA in each fraction by densitometry.

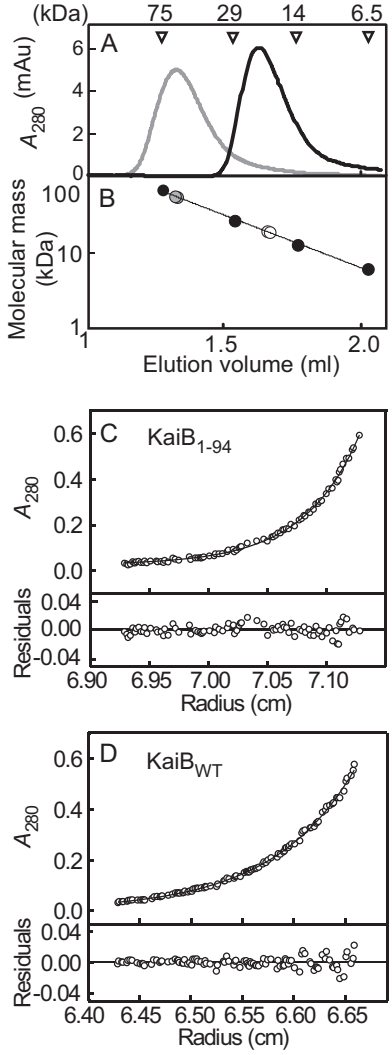


FIGURE 1. **Determination of the oligomeric state of $KaiB_{1-94}$ and $KaiB_{WT}$.** *A*, elution profiles of $KaiB_{1-94}$ and $KaiB_{WT}$ by gel filtration chromatography are shown. $KaiB_{1-94}$ and $KaiB_{WT}$ (the control) were subjected to analytical gel filtration chromatography at 4 °C on a Superdex75 5/150GL column equilibrated with 20 mM Tris-HCl buffer (pH 7.5) containing 150 mM NaCl. The elution positions of the molecular mass standards, conalbumin (75 kDa), carbonic anhydrase (29 kDa), ribonuclease (14 kDa), and aprotinin (6.5 kDa) are indicated *above the elution profiles*. Typical elution profiles from three independent experiments are shown. *Black line*, $KaiB_{1-94}$; *gray line*, $KaiB_{WT}$. *mAu*, milliabsorbance units. *B*, molecular masses of $KaiB_{1-94}$ and $KaiB_{WT}$ were determined by gel filtration chromatography. *Open circles*, $KaiB_{1-94}$; *gray circles*, $KaiB_{WT}$; *closed circles*, the molecular mass standards. *C* and *D*, shown are sedimentation equilibrium analyses of $KaiB_{1-94}$ and $KaiB_{WT}$. The *upper panels* show the equilibrium profiles (○) displayed as the $A_{280}$ (*Au*) *versus* the radial distance and theoretical concentration profiles (*solid line*) for a single molecular species with a molecular mass of 22 and 48 kDa, respectively. The *lower panels* show the residual plots from the curve fitting. *C*, $KaiB_{1-94}$; *D*, $KaiB_{WT}$.

## RESULTS

*Oligomeric Structures of $KaiB_{1-94}$ and $KaiB_{WT}$ in Solution*—To determine the oligomeric structure of $KaiB_{1-94}$ in solution, we estimated the molecular mass of $KaiB_{1-94}$ by gel filtration chromatography in gel filtration buffer. $KaiB_{1-94}$ (subunit molecular mass, 10.9 kDa) eluted as a single peak (Fig. 1*A*) corresponding to a 23.4 ± 0.4-kDa protein (Fig. 1*B* and Table 1) that corresponds to the approximate molecular mass of a dimer, whereas $KaiB_{WT}$ (subunit molecular mass, 12.4 kDa)

**TABLE 1**

**Molecular mass of $KaiB_{1–94}$**

GF, gel filtration chromatography; SE, sedimentation equilibrium analysis; GFB, gel filtration buffer; SEB, sedimentation equilibrium buffer. Values for gel filtration chromatography are the means ± S.D. from triplicate measurements.

| KaiB | Method | Buffer | Molecular mass ($n = 3$) |
|---|---|---|---|
| | | | *kDa* |
| $KaiB_{WT}$ | GF | GFB | 55.4 ± 0.6 |
| | GF | SEB | 56.0 ± 1.0 |
| $KaiB_{1–94}$ | GF | GFB | 23.4 ± 0.4 |
| | GF | SEB | 22.1 ± 0.4 |
| | GF | 20 mM Tris-HCl (pH 7.5), 50 mM NaCl | 22.5 ± 0.1 |
| | GF | 20 mM Tris-HCl (pH 7.5), 500 mM NaCl | 25.6 ± 0 |
| | GF | 20 mM MES-NaOH (pH 6.5), 150 mM NaCl | 24.0 ± 0.5 |
| | GF | 20 mM Tris-HCl (pH 8.5), 150 mM NaCl | 22.5 ± 0.5 |
| $KaiB_{WT}$ | SE | SEB | 49.8 |
| $KaiB_{1–94}$ | SE | SEB | 23.0 |

eluted as a single peak (Fig. 1*A*) corresponding to a 55.4 ± 0.6-kDa protein (Fig. 1*B* and Table 1) that corresponds to the approximate molecular mass of a tetramer. We obtained similar results under varying buffer conditions (Table 1). In sedimentation equilibrium analysis, $KaiB_{1–94}$ sedimented as a dimer with a molecular mass of 23 kDa (Fig. 1*C* and Table 1), and $KaiB_{WT}$ sedimented as a tetramer with a molecular mass of 48 kDa (Fig. 1*D* and Table 1), confirming the gel filtration chromatography results. Hereafter, when their concentrations are expressed, $KaiB_{WT}$ is considered a tetramer and $KaiB_{1–94}$ a dimer.

*Complex Formation of $KaiB_{1–94}$ and $KaiB_{WT}$ with KaiC and the Stoichiometry of the $KaiB_{1–94}$-$KaiC_{DD}$ and $KaiB_{WT}$-$KaiC_{DD}$ Complexes*—First, we examined the complex formation of $KaiB_{1–94}$ with $KaiC_{WT}$, $KaiC_{DD}$, and $KaiC_{AA}$ by FCS analysis (supplemental Fig. S1). The diffusion time of Cy3-$KaiB_{1–94}$ incubated alone at 25 °C for 18 h was 0.13 ± 0.04 ms, and it increased in the presence of $KaiC_{DD}$ (0.37 ± 0.09 ms). On the other hand, the diffusion time scarcely increased in the presence of $KaiC_{AA}$ (0.16 ± 0.03 ms). These results indicate that $KaiB_{1–94}$ formed a complex with $KaiC_{DD}$, whereas it scarcely formed a complex with $KaiC_{AA}$. Furthermore, the diffusion time of Cy3-$KaiB_{1–94}$ increased in the presence of $KaiC_{WT}$ when the phosphorylation level of $KaiC_{WT}$ had been elevated to about 70% by KaiA (0.26 ± 0.03 ms), whereas it increased only slightly in the presence of $KaiC_{WT}$ when the phosphorylation level of $KaiC_{WT}$ (about 30%) had not been elevated by KaiA (0.18 ± 0.03 ms). Therefore, the complex formation of $KaiB_{1–94}$ with KaiC depends on the phosphorylation level of KaiC; the higher the phosphorylation level, the more efficient complex formation occurred. Probably, $KaiB_{1–94}$ associates with p-KaiC more strongly than with np-KaiC. These results are consistent with a previous observation that $KaiB_{WT}$ associates with p-KaiC more strongly than with np-KaiC (30, 31). Hereafter, we used $KaiC_{DD}$ to examine the complex formation of KaiB with KaiC because the phosphorylation level of $KaiC_{WT}$ changes during incubation, especially in the presence of KaiB and/or KaiA (Ref. 4 and see Fig. 3*A*).

Next we examined the $KaiB_{1–94}$-$KaiC_{DD}$ complex by gel filtration chromatography followed by SDS-PAGE. $KaiB_{1–94}$ and $KaiC_{DD}$ each eluted as a single peak, $KaiB_{1–94}$ with an apparent molecular mass of 25 ± 2 kDa and $KaiC_{DD}$ with an apparent molecular mass of 319 ± 7 kDa ($n = 3$) (Fig. 2*A*). When $KaiC_{DD}$ (1 μM) was incubated with an excess of $KaiB_{1–94}$ (5 μM) at 40 °C for 18 h ($n = 3$), the reaction products eluted as two peaks, one with a molecular mass of 26 ± 1 kDa ($KaiB_{1–94}$) and the other with a molecular mass of 350 ± 20 kDa (Fig. 2*A*), suggesting the formation of a $KaiB_{1–94}$-$KaiC_{DD}$ complex. We also confirmed the formation of a $KaiB_{WT}$-$KaiC_{DD}$ complex (366 ± 20 kDa) by gel filtration chromatography (Fig. 2*A*). The apparent molecular masses of the $KaiB_{1–94}$-$KaiC_{DD}$ and $KaiB_{WT}$-$KaiC_{DD}$ complexes were slightly higher than that of the $KaiC_{DD}$ hexamer (Fig. 2*A*).

To determine the stoichiometry of the $KaiB_{1–94}$-$KaiC_{DD}$ complex, we collected it by gel filtration chromatography (Fig. 2*A*, 9.0–9.5 ml) and estimated the amount of $KaiB_{1–94}$ and $KaiC_{DD}$ it contained by SDS-PAGE (Fig. 2*B*) followed by densitometry (Fig. 2, *C* and *D*). When $KaiC_{DD}$ (1 μM) was incubated with an excess of $KaiB_{1–94}$ (5 μM) at 40 °C for 18 h, the fraction containing the complex contained 3.8 ± 0.3 subunits of $KaiB_{1–94}$ per molecule of hexameric $KaiC_{DD}$ (Fig. 2*E*). When we applied the same procedure to the $KaiB_{WT}$-$KaiC_{DD}$ complex, the stoichiometry showed that it contained 4.2 ± 0.4 subunits of $KaiB_{WT}$ per molecule of hexameric $KaiC_{DD}$ (Fig. 2*E*), indicating that the $KaiB_{1–94}$-$KaiC_{DD}$ complex consisted of two molecules of $KaiB_{1–94}$ (a dimer) and one molecule of hexameric $KaiC_{DD}$, whereas the $KaiB_{WT}$-$KaiC_{DD}$ complex consisted of one molecule of $KaiB_{WT}$ (a tetramer) and one molecule of hexameric $KaiC_{DD}$.

We confirmed these results using FCS with Cy3-NHS fluorescent dye ester (Cy3)-labeled KaiB proteins (Cy3-$KaiB_{1–94}$ and Cy3-$KaiB_{WT}$). When 0.2 μM Cy3-$KaiB_{1–94}$ and 0.1 μM Cy3-$KaiB_{WT}$ were incubated in the presence of 0, 0.025, 0.05, 0.15, or 0.3 μM $KaiC_{DD}$, the diffusion time varied directly with the $KaiC_{DD}$ concentration (Fig. 2*F*), indicating complex formation between $KaiC_{DD}$ and Cy3-$KaiB_{1–94}$ or Cy3-$KaiB_{WT}$.

The counts per particle of Cy3-$KaiB_{1–94}$ (0.2 μM) also varied with $KaiC_{DD}$ concentration (Fig. 2*G*). The counts per particle values of Cy3-$KaiB_{1–94}$ in the presence of $KaiC_{DD}$ at molar ratios greater than 0.5 were approximately twice those in its absence, which suggested that one molecule of the Cy3-$KaiB_{1–94}$-$KaiC_{DD}$ complex contained two molecules of the Cy3-$KaiB_{1–94}$ dimer (Fig. 2*G*). In contrast, counts per particle did not significantly change when Cy3-$KaiB_{WT}$ (0.1 μM) was incubated with an excess of $KaiC_{DD}$ (0.3 μM), which suggests that one molecule of the $KaiB_{WT}$-$KaiC_{DD}$ complex contained one molecule of the $KaiB_{WT}$ tetramer (Fig. 2*G*).

*Interaction of $KaiB_{1–94}$ Versus $KaiB_{WT}$ with $KaiC_{DD}$*—Surface plasmon resonance analysis showed that the association rate ($k_a$) of $KaiC_{DD}$ was 8 times as high with $KaiB_{1–94}$ as with $KaiB_{WT}$, and its dissociation rate ($k_d$) was 0.6 times as high (Table 2). Thus, the binding affinity of $KaiB_{1–94}$ for $KaiC_{DD}$ was 15 times the binding affinity of $KaiB_{WT}$. We also examined the binding affinities of KaiA and SasA, other known KaiC-binding proteins, and determined that $KaiB_{1–94}$ had the highest binding affinity in the group (Table 2).

*Circadian Oscillations in the Level of p-KaiC in an in Vitro KaiABC Clock System and Circadian Gene Expression Rhythms in T. elongatus Cells*—When 0.5 μM KaiA, KaiB ($KaiB_{1–94}$ or $KaiB_{WT}$), KaiC, and ATP were incubated together at 25 or 40 °C

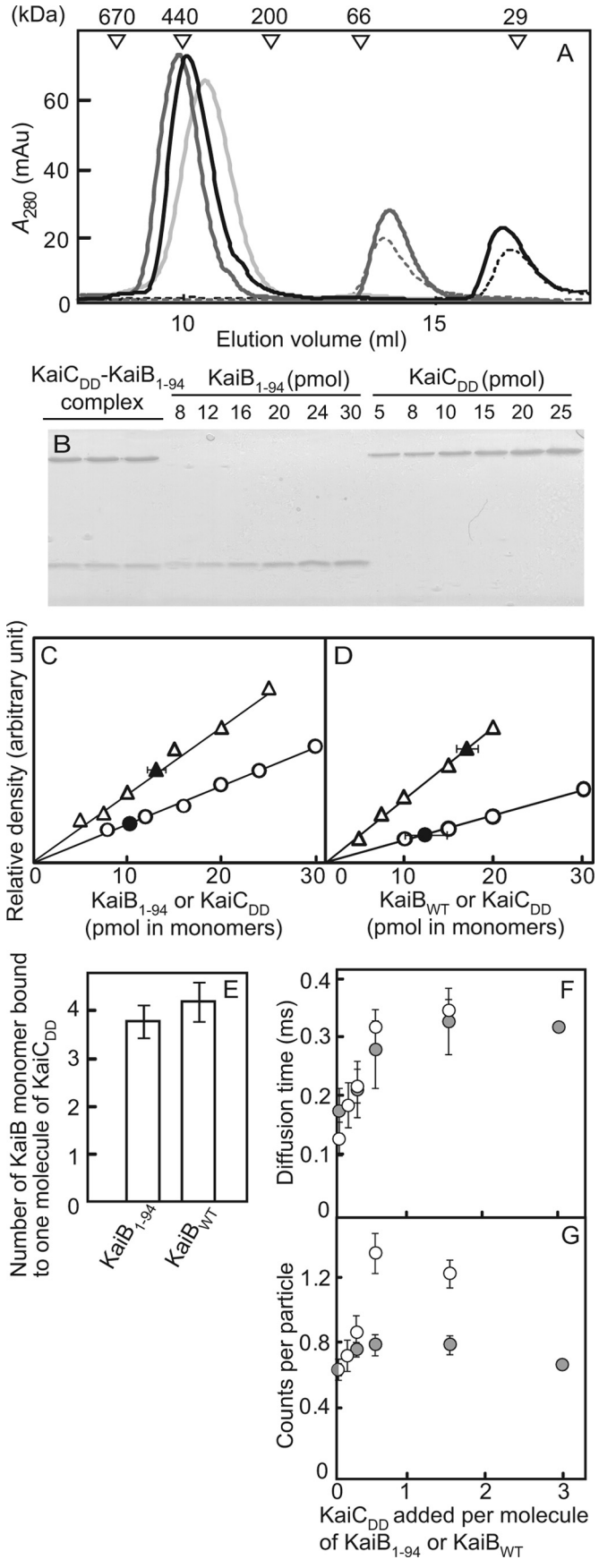


**TABLE 2**

**Kinetic and steady state parameters for the interaction of $KaiB_{WT}$, $KaiB_{1-94}$, KaiA, and SasA with $KaiC_{DD}$ obtained by surface plasmon resonance analysis**

Values are the means ± S.D. from triplicate measurements.

| Protein | $k_a$ | $k_d$ | $K_D$ |
|---|---|---|---|
| | $M^{-1}s^{-1}$ ($\times 10^4$) | $s^{-1}$ ($\times 10^{-3}$) | $M$ ($\times 10^{-8}$) |
| $KaiB_{WT}$ | 1.3 ± 0.057 | 0.46 ± 0.058 | 3.5 ± 0.38 |
| $KaiB_{1-94}$ | 10.4 ± 0.61 | 0.26 ± 0.040 | 0.24 ± 0.029 |
| KaiA | 3.9 ± 1.0 | 2.5 ± 0.10 | 6.8 ± 1.4 |
| SasA | 7.7 ± 1.1 | 1.2 ± 0.066 | 1.5 ± 0.24 |

in an *in vitro* KaiABC clock system (4), the level of p-KaiC oscillated in the presence of $KaiB_{1-94}$ and $KaiB_{WT}$ (Fig. 3*A*). At 40 °C, the period length was 21.7 ± 0.9 h for the oscillations driven by $KaiB_{1-94}$ and 22.6 ± 0.2 h for those driven by $KaiB_{WT}$ (Fig. 3*A*), which was consistent with the circadian oscillations observed in *T. elongatus* cells (24.4 ± 0.3 h) (Ref. 16 and Fig. 3*B*). Thus, $KaiB_{1-94}$, like $KaiB_{WT}$, can generate circadian oscillations in the *in vitro* KaiABC clock system. At 25 °C, the period length was 21.7 ± 1.3 h for the oscillations driven by $KaiB_{1-94}$ and 23.3 ± 0.5 h for those driven by $KaiB_{WT}$ (Fig. 3*A*), indicating that the period lengths were temperature-compensated in our system.

Circadian rhythms were normal in the *kaiB*-null host cells carrying $kaiB_{WT}$ but showed a greatly reduced amplitude in those carrying $kaiB_{1-94}$ (Fig. 3*B*).

*Inhibition of SasA-$KaiC_{DD}$ Complex Formation by $KaiB_{1-94}$ and $KaiB_{WT}$*—To determine why cyanobacterial cells expressing $KaiB_{1-94}$ showed weakened circadian gene expression rhythms even though $KaiB_{1-94}$ is able to generate normal cir-

FIGURE 2. **Stoichiometry of the KaiB-KaiC complex and the formation of the KaiB-KaiC complex analyzed by FCS analysis.** *A*, shown are elution profiles. Reaction mixtures containing 5 μM $KaiB_{1-94}$ or 2.5 μM $KaiB_{WT}$ and 1 μM $KaiC_{DD}$ were incubated at 40 °C for 18 h in HEPES reaction buffer and then subjected to gel filtration chromatography. *Black line*, $KaiB_{1-94}$ + $KaiC_{DD}$; *gray line*, $KaiB_{WT}$ + $KaiC_{DD}$; *light gray line*, $KaiC_{DD}$; *black dotted line*, $KaiB_{1-94}$; *gray dotted line*, $KaiB_{WT}$. *mAu*, milliabsorbance units. *B*, shown is SDS-PAGE. Aliquots of a fraction containing the $KaiB_{1-94}$-$KaiC_{DD}$ complex or the $KaiB_{WT}$-$KaiC_{DD}$ complex were subjected to SDS-PAGE. Standard amounts of $KaiB_{1-94}$, $KaiB_{WT}$, and $KaiC_{DD}$ were also applied to the gels. Only the SDS-PAGE gel of the $KaiB_{1-94}$-$KaiC_{DD}$ complex is shown. *Lanes 1–3*, triplicate samples from the fraction containing the $KaiB_{1-94}$-$KaiC_{DD}$ complex; *lanes 4–9* contain 5–40 pmol of $KaiB_{1-94}$; *lanes 10–15* contain 5–40 pmol of $KaiC_{DD}$. *C*, shown are calibration curves for the $KaiB_{1-94}$-$KaiC_{DD}$ complex. The relative intensities of the bands were plotted against known amounts of $KaiB_{1-94}$ and $KaiC_{DD}$, and the $KaiB_{1-94}$ and $KaiC_{DD}$ bands from the $KaiB_{1-94}$-$KaiC_{DD}$ complex were plotted. Typical plots from three independent experiments are shown. *Open circles*, known amounts of $KaiB_{1-94}$; *open triangles*, known amounts of $KaiC_{DD}$; *closed circles* and *closed triangles*, $KaiB_{1-94}$ and $KaiC_{DD}$ in the complex, respectively. *D*, calibration curves for the $KaiB_{WT}$-$KaiC_{DD}$ complex are shown. The relative intensities of the bands were plotted against known amounts of $KaiB_{WT}$ and $KaiC_{DD}$, and the $KaiB_{WT}$ and $KaiC_{DD}$ bands from the $KaiB_{WT}$-$KaiC_{DD}$ complex were plotted. Typical plots from three independent experiments are shown. *Open circles*, known amounts of $KaiB_{WT}$; *open triangles*, known amounts of $KaiC_{DD}$; *closed circles* and *closed triangles*, $KaiB_{WT}$ and $KaiC_{DD}$ in the complex, respectively. *E*, stoichiometry of the KaiB-$KaiC_{DD}$ complex is shown. The number of molecules of $KaiB_{1-94}$ or $KaiB_{WT}$ monomer per molecule of $KaiC_{DD}$ contained in the KaiB-$KaiC_{DD}$ complex was estimated from the plots shown in *A–D*. Values shown are the means ± S.D. *F*, $KaiC_{DD}$-induced changes in the diffusion times of Cy3-$KaiB_{1-94}$ and Cy3-$KaiB_{WT}$ molecules are shown. Cy3-$KaiB_{1-94}$ (0.2 μM) and Cy3-$KaiB_{WT}$ (0.1 μM) were separately incubated with 0, 0.025, 0.05, 0.15, and 0.3 μM $KaiC_{DD}$, and their diffusion times were measured by FCS analysis. Values shown are the means ± S.D. from quadruple measurements. *Open circles*, Cy3-$KaiB_{1-94}$; *gray circles*, Cy3-$KaiB_{WT}$. *G*, $KaiC_{DD}$-induced changes in the counts per particle for the Cy3-$KaiB_{1-94}$ and Cy3-$KaiB_{WT}$ molecules are shown. The counts per particle were calculated from the data shown in *F*.

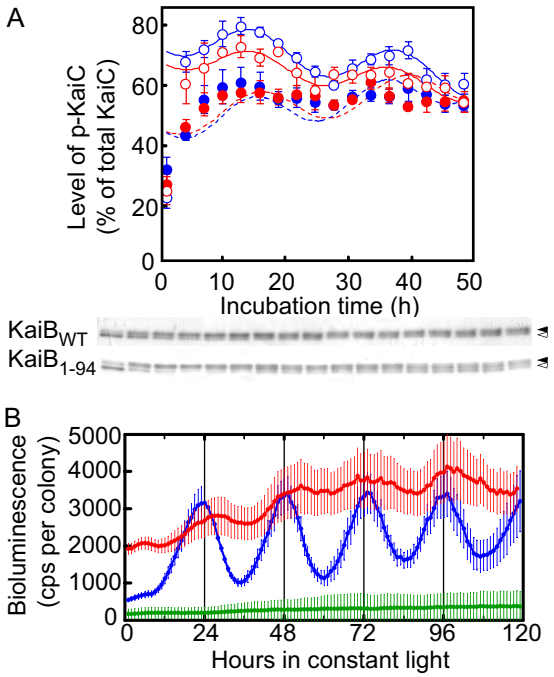


FIGURE 3. **Circadian oscillations *in vitro* and *in vivo*.** *A*, shown are circadian oscillations *in vitro*. Generation of temperature-compensated circadian oscillations *in vitro* in the level of p-KaiC by KaiB$_{1-94}$ in an *in vitro* KaiABC clock system is shown. Reaction mixtures containing KaiA, KaiB$_{WT}$ or KaiB$_{1-94}$, and KaiC$_{WT}$ (0.5 $\mu$M each) were incubated in 20 mM Tris-HCl buffer (pH 7.5) containing 1 mM ATP, 5 mM $MgCl_2$, and 150 mM NaCl at 25 °C or 40 °C for the periods indicated and were subjected to SDS-PAGE on 12.5% gels. The gels were stained with CBB, and the relative amounts of np-KaiC and p-KaiC were estimated by densitometry. Typical photographs from three independent experiments are shown. Circadian oscillations in the level of p-KaiC were analyzed by RAP, and the simulated curves are shown. Values shown are the means ± S.D. from triplicate measurements. KaiBs added: *open red circles*, KaiB$_{1-94}$ (40 °C); *open blue circles*, KaiB$_{WT}$ (40 °C); *closed red circles*, KaiB$_{1-94}$ (25 °C); *closed blue circles*, KaiB$_{WT}$ (25 °C). *Closed arrows*, p-KaiC; *open arrows*, np-KaiC. *B*, shown are circadian bioluminescence rhythms of a *T. elongatus* P$_{psbA1}$::Xl *luxAB* reporter strain carrying *kaiB*$_{WT}$ or *kaiB*$_{1-94}$ in a *kaiB*-null genetic background. Bioluminescence rhythms of *T. elongatus* P$_{psbA1}$::Xl *luxAB* reporter strains carrying *kaiB*$_{WT}$ (WT, *blue*, $n = 10$), *kaiB*$_{1-94}$ (KaiB$_{1-94}$, *red*, $n = 13$), and no additional *kaiB* gene (KaiB-null, *green*, $n = 75$) in a *kaiB*-null background (the *kaiB* gene had a nonsense codon just downstream of its initiation codon) were measured at 41 °C. Data points and *error bars* indicate the mean ± S.D. from *n* independent samples. *cps*, counts per s.

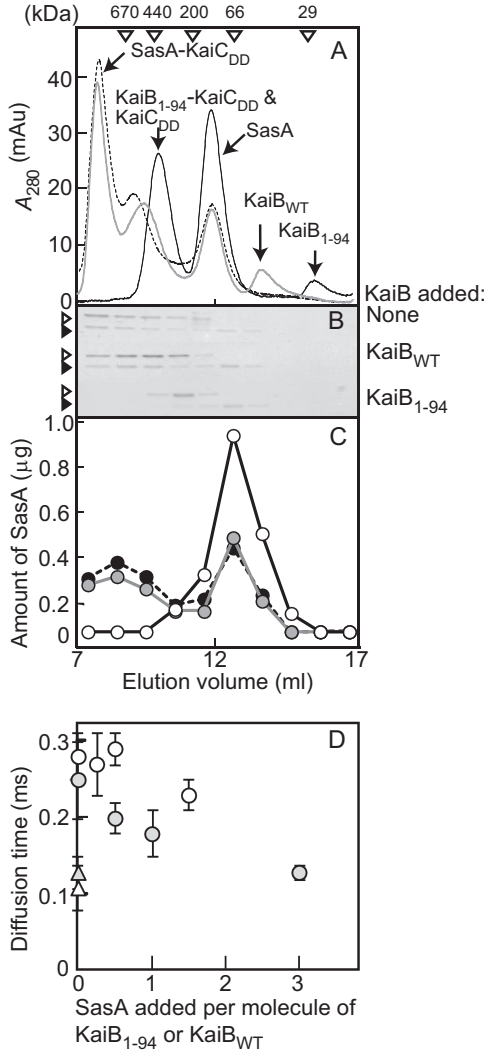


FIGURE 4. **Inhibition of the complex formation of SasA with KaiC$_{DD}$ by KaiB$_{1-94}$ and KaiB$_{WT}$.** *A*, elution profiles of gel filtration chromatography are shown. Reaction mixtures containing 1.5 $\mu$M SasA and 0.6 $\mu$M KaiC$_{DD}$ in HEPES reaction buffer containing 0.1 mM DTT were incubated in the presence or absence of 6.0 $\mu$M KaiB$_{1-94}$ or 3.0 $\mu$M KaiB$_{WT}$ at 25 °C for 18 h and were analyzed by gel filtration chromatography. Other conditions were as described in the Fig. 2 legend. Typical plots from three independent experiments are shown. KaiBs added: *black solid line*, KaiB$_{1-94}$; *gray solid line*, KaiB$_{WT}$; *black dotted line*, none. *mAu*, milliabsorbance units. *B*, shown is SDS-PAGE. Aliquots of the fractions (elution volumes, 7–17 ml) were subjected to SDS-PAGE on 15% gels, and the gels were visualized by CBB staining. *Open arrowheads* indicate KaiC$_{DD}$, and *closed arrowheads* indicate SasA. *C*, shown is the amount of SasA. The amount of SasA in each fraction was estimated with SDS-PAGE (Fig. 4*B*) using densitometry. KaiBs added: *closed circles* and *black dotted line*, none; *open circles* and *black solid line*, KaiB$_{1-94}$; *gray circles* and *gray solid line*, KaiB$_{WT}$. *D*, shown are SasA-induced changes in the diffusion times of the Cy3-KaiB$_{1-94}$ molecule and the Cy3-KaiB$_{WT}$ molecule in the presence of KaiC$_{DD}$. Reaction mixtures containing Cy3-KaiB (0.2 $\mu$M Cy3-KaiB$_{1-94}$ or 0.1 $\mu$M Cy3-KaiB$_{WT}$) and 0.1 $\mu$M KaiC$_{DD}$ were incubated in the presence or absence of the indicated amounts of SasA in HEPES reaction buffer containing 0.1 mM DTT at 25 °C for 18 h, and then the diffusion time was measured. The diffusion times of Cy3-KaiB$_{1-94}$ and Cy3-KaiB$_{WT}$ in the absence of KaiC$_{DD}$ and SasA were measured as controls. Values shown are the means ± S.D. from quadruple measurements. Other conditions were the same as described in the Fig. 2*F* legend. *Open circles*, Cy3-KaiB$_{1-94}$; *open triangles*, Cy3-KaiB$_{1-94}$ without KaiC$_{DD}$ and SasA; *gray circles*, Cy3-KaiB$_{WT}$; *gray triangles*, Cy3-KaiB$_{WT}$ without KaiC$_{DD}$ and SasA.

cadian oscillations *in vitro*, we examined the effects of KaiB on the SasA-mediated clock output pathway, that is, on the formation of the SasA-KaiC complex.

Gel filtration chromatography yielded only a single peak for both KaiC$_{DD}$ and SasA corresponding to a 340 ± 20-kDa protein and a 140 ± 10-kDa protein, respectively. When reaction mixtures containing 1.5 $\mu$M SasA and 0.6 $\mu$M KaiC$_{DD}$ were incubated in the absence or presence of 3 $\mu$M KaiB$_{WT}$ or 6 $\mu$M KaiB$_{1-94}$ at 25 °C for 18 h, the elution profile of the sample without KaiB showed 3 peaks (Fig. 4*A*) that we analyzed by SDS-PAGE (Fig. 4*B*). Peak 1 (>670 kDa, the molecular mass of the largest standard used) corresponded to the SasA-KaiC$_{DD}$ complex, peak 2 (440 ± 50 kDa) corresponded to the other form of the SasA-KaiC$_{DD}$ complex, and peak 3 (130 ± 5 kDa) corresponded to SasA. The amount of SasA contained in each fraction estimated by SDS-PAGE followed by densitometry showed that 34 ± 10% ($n = 3$) of the total SasA was unbound (Fig. 4*C*).

The elution profile of the sample with 6 $\mu$M KaiB$_{1-94}$ showed three peaks (Fig. 4*A*); peak 1 (360 ± 10 kDa) corresponded to KaiC$_{DD}$ and the KaiB$_{1-94}$-KaiC$_{DD}$ complex, peak 2 (140 ± 10 kDa) corresponded to SasA, and peak 3 (20 ± 0 kDa) corresponded to KaiB$_{1-94}$. The presence of KaiB$_{1-94}$ all but extin-

guished the SasA-$KaiC_{DD}$ complex and greatly increased free SasA (Fig. 4*A*). The free SasA fractions contained 92 ± 10% ($n = 3$) of the total SasA added (Fig. 4, *B* and *C*), which indicated nearly complete inhibition of SasA-$KaiC_{DD}$ complex formation by $KaiB_{1-94}$. In the presence of 3 μM $KaiB_{WT}$, the elution profile of the sample showed four peaks (Fig. 4*A*) corresponding to the SasA-$KaiC_{DD}$ complex (>670 kDa), the other form of the SasA-$KaiC_{DD}$ complex, $KaiC_{DD}$ and $KaiB_{WT}$-$KaiC_{DD}$ complex (420 ± 40 kDa), SasA (140 ± 10 kDa), and $KaiB_{WT}$ (50 ± 0 kDa). The presence of $KaiB_{WT}$ slightly reduced the SasA-$KaiC_{DD}$ complex peak and slightly increased the free SasA peak; the free SasA fractions contained 43 ± 5% ($n = 3$) of the total SasA added (control 34 ± 10%) (Fig. 4*C*), which suggests that $KaiB_{WT}$ inhibited formation of the SasA-$KaiC_{DD}$ complex, albeit very slightly. Thus, $KaiB_{1-94}$ was a stronger inhibitor of SasA-$KaiC_{DD}$ complex formation than $KaiB_{WT}$.

We also examined KaiB inhibition of SasA-$KaiC_{WT}$ complex formation by FCS analysis with Cy3-SasA (supplemental Fig. S2). The diffusion time of Cy3-SasA (0.2 μM) incubated alone at 25 °C for 18 h was 0.14 ± 0.00 ms. On the other hand, when Cy3-SasA was incubated with 0.2 μM $KaiC_{WT}$, its diffusion time increased to 0.30 ± 0.06 ms, indicating formation of a Cy3-SasA-$KaiC_{WT}$ complex. The addition of 2.0 μM $KaiB_{1-94}$ almost completely canceled this diffusion time increase (0.16 ± 0.03 ms), indicating that $KaiB_{1-94}$ inhibited SasA-$KaiC_{WT}$ complex formation as well as SasA-$KaiC_{DD}$ complex formation (see above). However, the addition of $KaiB_{WT}$ did not cancel the diffusion time increase under the conditions examined (diffusion time: 0.35 ± 0.03 and 0.33 ± 0.01 ms in the presence of 1.0 μM $KaiB_{WT}$ and 2.0 μM $KaiB_{WT}$, respectively) (supplemental Fig. S2).

We examined SasA inhibition of KaiB-$KaiC_{DD}$ complex formation by FCS analysis with Cy3-$KaiB_{1-94}$ and Cy3-$KaiB_{WT}$ (Fig. 4*D*). In the absence of $KaiC_{DD}$, the diffusion time was 0.13 ± 0.02 ms for 0.2 μM Cy3-$KaiB_{1-94}$ and 0.11 ± 0.03 ms for 0.1 μM Cy3-$KaiB_{WT}$. In the presence of 0.1 μM $KaiC_{DD}$, it increased to 0.28 ± 0.03 ms for Cy3-$KaiB_{1-94}$ and 0.25 ± 0.05 ms for Cy3-$KaiB_{WT}$ (Fig. 4*D*), indicating formation of the Cy3-$KaiB_{1-94}$-$KaiC_{DD}$ and Cy3-$KaiB_{WT}$-$KaiC_{DD}$ complexes. The diffusion time of 0.2 μM Cy3-$KaiB_{1-94}$ was slightly shorter in the presence of 0.3 μM SasA (0.23 ± 0.02 ms) than in its absence (0.28 ± 0.03) (Fig. 4*D*), which indicates that SasA weakly inhibited formation of the $KaiB_{1-94}$-$KaiC_{DD}$ complex. In the presence of $KaiC_{DD}$, on the other hand, SasA reduced the diffusion time of 0.1 μM Cy3-$KaiB_{WT}$ from 0.25 ± 0.05 to 0.13 ± 0.01 ms, the level it was in the absence of $KaiC_{DD}$ (0.11 ± 0.03 ms) (Fig. 4*D*), which indicates that SasA almost completely inhibited formation of the $KaiB_{WT}$-$KaiC_{DD}$ complex. Thus, SasA inhibited $KaiB_{WT}$-$KaiC_{DD}$ complex formation more strongly than $KaiB_{1-94}$-$KaiC_{DD}$ complex formation.

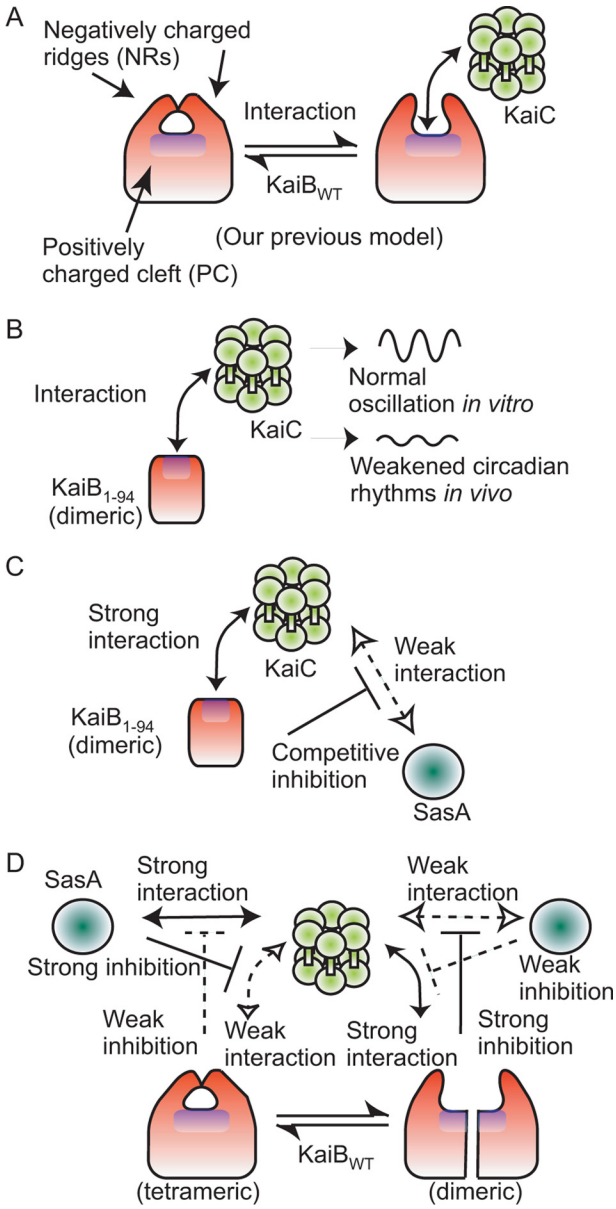


FIGURE 5. **Model for the conformational change of KaiB.** On one surface of the KaiB tetramer, a PC is covered with two NRs, and the active sites (16) and KaiA-interacting site (17) are located on the PC. Therefore, we hypothesize that the PC is exposed for ligand binding by NR movement (Refs. 16 and 39; *A*). The PC on $KaiB_{1-94}$, on the other hand, is always exposed, which allows it to interact with KaiC because it lacks the NRs and exists as a dimer (*B*). $KaiB_{1-94}$ is more stable than $KaiB_{WT}$ as a binding partner for KaiC, which suggests that the KaiB binding site is located on the PC and that the PC may be exposed to KaiC by NR movement (*A*). Thus, $KaiB_{1-94}$ competitively inhibits the interaction of SasA with KaiC by its strong interaction with KaiC, which is necessary for the generation of normal circadian gene expression rhythms in cyanobacterial cells (*C*). On interaction with KaiC, the KaiB tetramer molecule may dissociate into two dimeric molecules that bind to one hexameric KaiC molecule (*D*). The tetrameric structure and NRs of the KaiB molecule are necessary for normal circadian gene expression rhythms in cells (*D*) but not for circadian oscillations in the *in vitro* KaiABC clock system.

## DISCUSSION

That $KaiB_{1-94}$ is a dimer (Fig. 1 and Table 1) but interacts with $KaiC_{DD}$ in much the same way as tetrameric $KaiB_{WT}$ (Fig. 2) and can generate normal circadian oscillations *in vitro* (Fig. 3*A*) indicates that KaiB tetramericity is not required for the generation of circadian oscillations *per se*. The tetrameric structure of KaiB, however, and its negatively charged C-terminal region seem to play an important role in the generation of circadian gene expression rhythms *in vivo* because the circadian bioluminescence rhythms of cyanobacterial cells expressing $KaiB_{1-94}$ in a Δ*kaiB* genetic background are greatly weakened (Ref. 16 and Fig. 3*B*). We demonstrated that whereas $KaiB_{WT}$ inhibits the formation of the SasA-KaiC complex

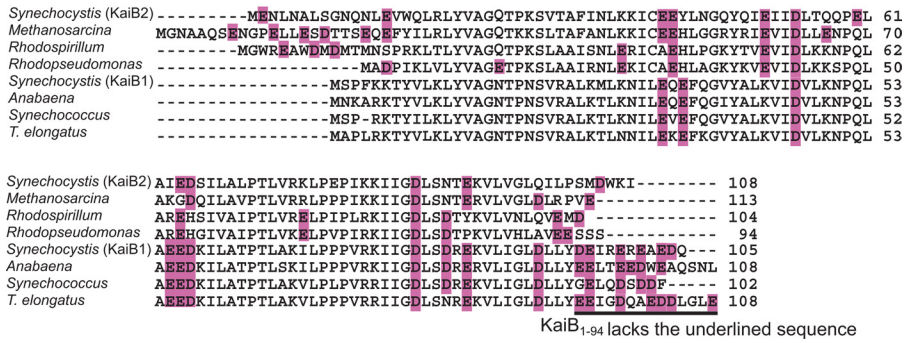


FIGURE 6. **Amino acid sequence alignment of KaiB.** We aligned the amino acid sequences of KaiB from three strains of cyanobacteria, two strains of archaea, and two strains of green-sulfur bacteria using ClustalX (42). The negatively charged residues (glutamate and aspartate are *shaded in purple*). The C-terminal deletion in $KaiB_{1-94}$ is indicated by *underlining*. Cyanobacterial strains: *Synechococcus* sp. strain PCC 7942; *T. elongatus* BP-1; *Anabaena* sp. strain PCC 7120; *Synechocystis* sp. PCC 6803 KaiB1; *Synechocystis* sp. PCC 6803 KaiB2. Archaeal strain: *Methanosarcina mazei Goe1*. Proteobacterial strains: *Rhodospirillum rubrum* ATCC 11170; *Rhodopseudomonas palustris* CGA009.

slightly, $KaiB_{1-94}$ inhibits it strongly (Fig. 4 and supplemental Fig. S2), probably because of the high affinity of $KaiB_{1-94}$ for $KaiC_{DD}$ (Table 2).

SasA is a KaiC binding histidine kinase in the SasA-RpaA two-component regulatory system (32, 33) and is involved in the main clock output pathway. Ultimately, the time information of the KaiABC clock oscillator is transmitted to the transcription apparatus and generates genome-wide circadian transcription rhythms in cyanobacteria. Disruption of the *sasA* gene greatly lowers the level of *kaiBC* expression and the amplitude of *kaiA* and *kaiBC* expression rhythms (32). $KaiB_{1-94}$ competitively inhibits the SasA-KaiC interaction more strongly than $KaiB_{WT}$ does due to its higher affinity for KaiC (Table 2); it is likely, therefore, that $KaiB_{1-94}$ hinders the SasA-KaiC interaction that is necessary for the transmission of the time information from the KaiABC clock oscillator to the transcription apparatus through the SasA-mediated clock output pathway (32, 33). We hypothesize that the defective rhythm phenotypes of cyanobacterial cells expressing $KaiB_{1-94}$ in a Δ*kaiB* genetic background follow from a $KaiB_{1-94}$-induced defect in the SasA-KaiC interaction involved in the SasA-mediated clock output pathway.

KaiB ($KaiB_{1-94}$ and $KaiB_{WT}$) inhibited formation of the SasA-KaiC ($KaiC_{DD}$ and $KaiC_{WT}$) complex (Fig. 4, *A–C*, and supplemental Fig. S2), and SasA inhibited formation of the KaiB ($KaiB_{1-94}$ and $KaiB_{WT}$)-$KaiC_{DD}$ complex (Fig. 4*D*). It is unknown whether the two proteins compete for an identical binding site on KaiC because the binding sites of KaiB and SasA on KaiC are not determined. Previously, the N-terminal domain of SasA was suggested to be homologous to KaiB (32). However, comparison between the NMR structure of SasA N-terminal domain and the x-ray crystal structure of KaiB demonstrated that KaiB and SasA N-terminal domain have different folds (34). Therefore, it is not likely that SasA and KaiB bind to the same site on KaiC. We have demonstrated by surface plasmon resonance analysis and gel filtration chromatography that the SasA binding site of KaiC is located on its N-terminal domain (21), as suggested by NMR analysis (35). The SasA inhibition of $KaiB_{WT}$-$KaiC_{WT}$ complex formation has been demonstrated by Native-PAGE using proteins derived from *Synechococcus* (36).

Our demonstration that two molecules of $KaiB_{1-94}$ bind to one molecule of $KaiC_{DD}$ (Fig. 2) suggests that two molecules of $KaiB_{1-94}$ dimer bind to one molecule of a KaiC hexamer. Because one molecule of $KaiB_{WT}$ binds to one molecule of $KaiC_{DD}$ (Fig. 2), it is likely that upon interaction with KaiC, the KaiB molecule changes from a tetramer to a dimer. This is consistent with the cryo-electron microscopy analysis of the $KaiB_{WT}$-$KaiC_{WT}$ complex that revealed the possibility of KaiB binding to KaiC as two dimers (37). Based on the crystal structure of KaiB, we have proposed that the interdimer interface of the KaiB tetrameric molecule could be destabilized by changes in pH or ionic strength and dissociate into two dimers (16).

On one surface of the KaiB tetramer, a PC, which is the active site, is covered with two NRs, and the PC may be exposed for ligand binding by NR movement (Fig. 5*A*) (16). In agreement with this model, $KaiB_{1-94}$, which lacks NRs and has a continuously exposed PC, is a more stable binding partner for $KaiC_{DD}$ than $KaiB_{WT}$ (Table 2). It is likely that PC exposure by NR movement may play an important role in the interaction of KaiB with KaiC (Fig. 5, *A* and *B*). An alternative model is that KaiB associates with KaiC using a surface, which is exposed by the deletion of NRs on KaiB or the dimerization of KaiB. There are two areas on KaiC that are highly negatively charged, one around the pore opening and inside the pore of KaiC N-terminal domain and the other around the intersubunit interface of one of two adjacent KaiC N-terminal domains (Ref. 38 and supplemental Fig. S3). Possible electrostatic interaction between the PC on KaiB and the negatively charged surfaces of KaiC might occur.

Our demonstration that the stable interaction of $KaiB_{1-94}$ with KaiC inhibited the interaction of SasA with KaiC (Fig. 4) indicated that the C-terminal region of KaiB is necessary for driving normal circadian transcription rhythms through regulation of the KaiC-SasA interaction (Fig. 5, *C* and *D*). Furthermore, our recent observations are consistent with our model as follows. Electron spin resonance analysis demonstrated that the mobility of the spin labels introduced into the amino acid residues located on the PC greatly increased on incubation at 40 °C (39), which indicates that the local structure surrounding the spin labels on the PC is relaxed during incubation (39); the 64th

residue located inside the KaiB molecule near the PC interacts with KaiA (17).

In the KaiABC clock oscillator, KaiA associates preferentially with np-KaiC (40) ($KaiC_{AA}$ mimics np-KaiC) to elevate the phosphorylation level of KaiC (11–13). Then, KaiA dissociates from the p-KaiC ($KaiC_{DD}$ mimics completely phosphorylated KaiC) (40). In contrast, KaiB associates preferentially with the p-KaiC (Ref. 6 and supplemental Fig. S1) and then reduces the phosphorylation level of KaiC (12, 14). A series of these reactions and interactions among Kai proteins generate circadian oscillations such as oscillations in the phosphorylation level (4) and ATPase activity (5) of KaiC and complex formation among Kai proteins (6, 7). SasA also associates preferentially with p-KaiC, which enhances the autophosphorylation of SasA (21). KaiB and SasA compete each other for KaiC (Fig. 4 and supplemental Fig. S2). Therefore, it is likely that KaiB regulates the normal SasA-KaiC interaction required for the transmission of time information from KaiC to the transcription apparatus, resulting in genome-wide transcription cycles in cyanobacterial cells (21, 32, 33). SasA trimer and KaiC hexamer associate each other at a 1:1 molar ratio at their N-terminal domains, and the phosphorylation states of their C-terminal domains affect the affinity of the interaction (21). Interestingly, the phosphorylation state of KaiC also affects the rigidity of the C-terminal domains of KaiC hexamer and the interaction between the N-terminal domains and C-terminal domains of the KaiC, and KaiC associates with KaiB when the structure of KaiC C-terminal domains is rigid (35).

KaiB and KaiC occur in Archaea and Proteobacteria as well as in cyanobacteria (41). The C-terminal cluster of negatively charged residues is highly conserved in cyanobacterial clock KaiBs (Ref. 16 and Fig. 6) but not in cyanobacterial non-clock KaiBs (such as *Synechocystis* KaiB2 (41)) and not in KaiB homologues in Archaea and Proteobacteria (Fig. 6). The negatively charged C terminus of KaiB likely plays an important role in the SasA-mediated clock output pathway through KaiB-KaiC interactions affecting the SasA-KaiC interaction. SasA is present only in cyanobacteria, which suggests that the negatively charged C-terminal region of cyanobacterial KaiB may have co-evolved with SasA as a component of the cyanobacterial circadian system.

*Acknowledgments—We thank Satoko Ogawa and Kumiko Tanaka for technical support and Miriam Bloom (SciWrite Biomedical Writing and Editing Services) for professional editing. Development of the automated bioluminescence monitoring apparatus CL96–4 and the plate conveyor robot CI-08L were supported by SENTAN, JST. The apparatuses CL96–4 and CI-08L are commercially available through Churitsu Electric Corp. (Nagoya, Japan).*

## REFERENCES

1. Bünning, E. (1973) *The Physiological Clock. Circadian Rhythms and Biological Chronometry*, 3rd Ed., Springer-Verlag, New York, NY
2. Sweeney, B. M., and Borgese, M. B. (1989) A circadian rhythm in cell division in a prokaryote, the cyanobacterium *Synechococcus* WH7803. *J. Phycol.* **25,** 183–186
3. Ishiura, M., Kutsuna, S., Aoki, S., Iwasaki, H., Andersson, C. R., Tanabe, A., Golden, S. S., Johnson, C. H., and Kondo, T. (1998) Expression of a gene cluster *kaiABC* as a circadian feedback process in cyanobacteria. *Science* **281,** 1519–1523
4. Nakajima, M., Imai, K., Ito, H., Nishiwaki, T., Murayama, Y., Iwasaki, H., Oyama, T., and Kondo, T. (2005) Reconstitution of circadian oscillation of cyanobacterial KaiC phosphorylation in vitro. *Science* **308,** 414–415
5. Terauchi, K., Kitayama, Y., Nishiwaki, T., Miwa, K., Murayama, Y., Oyama, T., and Kondo, T. (2007) ATPase activity of KaiC determines the basic timing for circadian clock of cyanobacteria. *Proc. Natl. Acad. Sci. U.S.A.* **104,** 16377–16381
6. Kageyama, H., Nishiwaki, T., Nakajima, M., Iwasaki, H., Oyama, T., Kondo, T. (2006) Cyanobacterial circadian pacemaker. Kai protein complex dynamics in the KaiC phosphorylation cycle in vitro. *Mol. Cell* **23,** 161–171
7. Akiyama, S., Nohara, A., Ito K., Maéda, Y. (2008) Assembly and disassembly dynamics of the cyanobacterial periodosome. *Mol. Cell* **29,** 703–716
8. Murakami, R., Miyake, A., Iwase, R., Hayashi, F., Uzumaki, T., and Ishiura, M. (2008) ATPase activity and its temperature compensation of the cyanobacterial clock protein KaiC. *Genes Cells* **13,** 387–395
9. Nishiwaki, T., Iwasaki, H., Ishiura, M., and Kondo, T. (2000) Nucleotide binding and autophosphorylation of the clock protein KaiC as a circadian timing process of cyanobacteria. *Proc. Natl. Acad. Sci. U.S.A.* **97,** 495–499
10. Hayashi, F., Iwase, R., Uzumaki, T., and Ishiura, M. (2006) Hexamerization by the N-terminal domain and intersubunit phosphorylation by the C-terminal domain of cyanobacterial circadian clock protein KaiC. *Biochem. Biophys. Res. Commun.* **348,** 864–872
11. Iwasaki, H., Nishiwaki, T., Kitayama, Y., Nakajima, M., and Kondo, T. (2002) KaiA-stimulated KaiC phosphorylation in circadian timing loops in cyanobacteria. *Proc. Natl. Acad. Sci. U.S.A.* **99,** 15788–15793
12. Williams, S. B., Vakonakis, I., Golden, S. S., and LiWang, A. C. (2002) Structure and function from the circadian clock protein KaiA of *Synechococcus elongatus*. A potential clock input mechanism. *Proc. Natl. Acad. Sci. U.S.A.* **99,** 15357–15362
13. Uzumaki, T., Fujita, M., Nakatsu, T., Hayashi, F., Shibata, H., Itoh, N., Kato, H., and Ishiura, M. (2004) Crystal structure of the C-terminal clock-oscillator domain of the cyanobacterial KaiA protein. *Nat. Struct. Mol. Biol.* **11,** 623–631
14. Kitayama, Y., Iwasaki, H., Nishiwaki, T., and Kondo, T. (2003) KaiB functions as an attenuator of KaiC phosphorylation in the cyanobacterial circadian clock system. *EMBO J.* **22,** 2127–2134
15. Hitomi, K., Oyama, T., Han, S., Arvai, A. S., and Getzoff, E. D. (2005) Tetrameric architecture of the circadian clock protein KaiB. A novel interface for intermolecular interactions and its impact on the circadian rhythm. *J. Biol. Chem.* **280,** 19127–19135
16. Iwase, R., Imada, K., Hayashi, F., Uzumaki, T., Morishita, M., Onai, K., Furukawa, Y., Namba, K., and Ishiura, M. (2005) Functionally important substructures of circadian clock protein KaiB in a unique tetramer complex. *J. Biol. Chem.* **280,** 43141–43149
17. Mutoh, R., Mino, H., Murakami, R., Uzumaki, T., Takabayashi, A., Ishii, K., and Ishiura, M. (2010) Direct interaction between KaiA and KaiB revealed by a site-directed spin labeling electron spin resonance analysis. *Genes Cells* **15,** 269–280
18. Yamaoka, T., Satoh, K., and Katoh, S. (1978) Photosynthetic activities of a thermophilic blue-green alga. *Plant Cell Physiol.* **19,** 943–954
19. Hayashi, F., Suzuki, H., Iwase, R., Uzumaki, T., Miyake, A., Shen, J. R., Imada, K., Furukawa, Y., Yonekura, K., Namba, K., and Ishiura, M. (2003) ATP-induced hexameric ring structure of the cyanobacterial circadian clock protein KaiC. *Genes Cells* **8,** 287–296
20. Hayashi, F., Itoh, N., Uzumaki, T., Iwase, R., Tsuchiya, Y., Yamakawa, H., Morishita, M., Onai, K., Itoh, S., and Ishiura, M. (2004) Roles of two ATPase-motif-containing domains in cyanobacterial circadian clock protein KaiC. *J. Biol. Chem.* **279,** 52331–52337
21. Valencia S., J., Bitou, K., Ishii, K., Murakami, R., Morishita, M., Onai, K., Furukawa, Y., Imada, K., Namba, K., and Ishiura, M. (2012) Phase-dependent generation and transmission of time information by the KaiABC circadian clock oscillator through SasA-KaiC interaction in cyanobacteria. *Genes Cells* **17,** 398–419
22. Laemmli, U. K. (1970) Cleavage of structural proteins during the assembly of the head of bacteriophage T4. *Nature* **227,** 680–685
23. Eigen, M., and Rigler, R. (1994) Sorting single molecules. Application to

diagnostics and evolutionary biotechnology. *Proc. Natl. Acad. Sci. U.S.A.* **91,** 5740–5747
24. Takahashi, Y., Okamoto, Y., Popiel, H. A., Fujikake, N., Toda, T., Kinjo, M., and Nagai, Y. (2007) Detection of polyglutamine protein oligomers in cells by fluorescence correlation spectroscopy. *J. Biol. Chem.* **282,** 24039–24048
25. Karlsson, R., Katsamba, P. S., Nordin, H., Pol, E., and Myszka, D. G. (2006) Analyzing a kinetic titration series using affinity biosensors. *Anal. Biochem.* **349,** 136–147
26. Okamoto, K., Onai, K., and Ishiura, M. (2005) RAP, an integrated program for monitoring bioluminescence and analyzing circadian rhythms in real time. *Anal. Biochem.* **340,** 193–200
27. Okamoto, K., Onai, K., Furusawa, T., and Ishiura, M. (2005) A portable integrated automatic apparatus for the real-time monitoring of bioluminescence in plants. *Plant Cell Environ.* **28,** 1305–1315
28. Onai, K., and Ishiura, M. (2005) *PHYTOCLOCK* 1 encoding a novel GARP protein essential for the *Arabidopsis* circadian clock. *Genes Cells* **10,** 963–972
29. Onai, K., Morishita, M., Itoh, S., Okamoto, K., and Ishiura, M. (2004) Circadian rhythms in the thermophilic cyanobacterium *Thermosynechococcus elongatus*. Compensation of period length over a wide temperature range. *J. Bacteriol.* **186,** 4972–4977
30. Nishiwaki, T., Satomi, Y., Nakajima, M., Lee, C., Kiyohara, R., Kageyama, H., Kitayama, Y., Temamoto, M., Yamaguchi, A., Hijikata, A., Go, M., Iwasaki, H., Takao, T., and Kondo, T. (2004) Role of KaiC phosphorylation in the circadian clock system of *Synechococcus elongatus* PCC 7942. *Proc. Natl. Acad. Sci. U.S.A.* **101,** 13927–13932
31. Xu, Y., Mori, T., Pattanayek, R., Pattanayek, S., Egli, M., and Johnson, C. H. (2004) Identification of key phosphorylation sites in the circadian clock protein KaiC by crystallographic and mutagenetic analyses. *Proc. Natl. Acad. Sci. U.S.A.* **101,** 13933–13938
32. Iwasaki, H., Williams, S. B., Kitayama, Y., Ishiura, M., Golden, S., S., and Kondo, T. (2000) A KaiC-interacting sensory histidine kinase, SasA, necessary to sustain robust circadian oscillation in cyanobacteria. *Cell* **101,** 223–233
33. Takai, N., Nakajima, M., Oyama, T., Kito, R., Sugita, C., Sugita, M., Kondo, T., and Iwasaki, H. (2006) A KaiC-associating SasA-RpaA two-component regulatory system as a major circadian timing mediator in cyanobacteria. *Proc. Natl. Acad. Sci. U.S.A.* **103,** 12109–12114
34. Vakonakis, I., Klewer, D. A., Williams, S. B., Golden, S. S., and LiWang, A. C. (2004) Structure of the N-terminal domain of the circadian clock-associated histidine kinase SasA. *J. Mol. Biol.* **342,** 9–17
35. Chang, Y. G., Kuo, N. W., Tseng, R., and LiWang, A. (2011) Flexibility of the C-terminal, or CII, ring of KaiC governs the rhythm of the circadian clock of cyanobacteria. *Proc. Natl. Acad. Sci. U.S.A.* **108,** 14431–14436
36. Pattanayek, R., Williams D. R., Rossi, G., Weigand, S., Mori T., Johnson, C. H., Stewart, P. L., and Egli, M. (2011) Combined SAXS/EM-based models of the *S. elongatus* post-translational circadian oscillator and its interactions with the output His-kinase SasA. *PLoS One* **6,** e23697
37. Pattanayek, R., Williams, D. R., Pattanayek, S., Mori, T., Johnson, C. H., Stewart, P. L., and Egli, M. (2008) Structural model of the circadian clock KaiB-KaiC complex and mechanism for modulation of KaiC phosphorylation. *EMBO J.* **27,** 1767–1778
38. Pattanayek, R., Wang, J., Mori, T., Xu, Y., Johnson, C. H., and Egli, M. (2004) Visualizing a circadian clock protein. Crystal structure of KaiC and functional insights. *Mol. Cell* **15,** 375–388
39. Mutoh, R., Mino, H., Murakami, R., Uzumaki, T., and Ishiura, M. (2011) Thermodynamically induced conformational changes of the cyanobacterial circadian clock protein KaiB. *Appl. Magn. Reson.* **40,** 525–534
40. Hayashi, F., Ito, H., Fujita, M., Iwase, R., Uzumaki, T., and Ishiura, M. (2004) Stoichiometric interactions between cyanobacterial clock proteins KaiA and KaiC. *Biochem. Biophys. Res. Commun.* **316,** 195–202
41. Aoki, S., and Onai, K. (2009) *Circadian clocks of Synechocystis sp. strain PCC 6803, Thermosynechococcus elongatus, Prochlorococcus spp., Trichodesmium spp., and other species. Bacterial Circadian Programs,* pp. 259–282 (Ditty, J. L., Mackey, S. R., and Johnson, C. H., eds) Springer-Verlag, Berlin
42. Thompson, J. D., Gibson, T. J., Plewniak, F., Jeanmougin, F., and Higgins, D. G. (1997) The CLUSTAL_X windows interface. Flexible strategies for multiple sequence alignment aided by quality analysis tools. *Nucleic Acids Res.* **25,** 4876–4882